A Method for Estimating Maximum Damage Caused by Sediment Disaster by Surveying with Artificial Satellite SAR Imagery

Shin-ichiro HAYASHI[1*], Shin'ya KATSURA[1], Mio KASAI[1], Nobutomo OSANAI[1], Takashi YAMADA[1], Tomomi MARUTANI[1], Tomoyuki NORO[2] and Joko KAMIYAMA[2]

[1] Research Faculty of Agriculture, Hokkaido University, (Kita 9, Nishi 9, Kita-ku, Sapporo, Hokkaido 0608589, Japan)
[2] National Institute for Land and Infrastructure Management, (Asahi 1, Tsukuba, Ibaraki 3050804, Japan)
*Corresponding author. E-mail: shayashi@cen.agr.hokudai.ac.jp

Estimating the maximum damage caused by sediment disasters is necessary for reducing the time required for determining critical risk management resources. In this study, we proposed a method for estimating maximum damage using the Sediment Disaster Scale (SDS); our method calculates the Sediment Movement Magnitude (SMM) , an index pertaining to sediment movement that is based on survey implementing synthetic aperture radar (SAR) imagery, that can be obtained even during bad weather and at night, and is extensively used within disaster surveys. We then evaluated and confirmed the applicability of our proposed method by comparing the maximum damage estimated from SAR imagery to the actual damage incurred. Our method reduces the time necessary for surveying compared with conventional disaster survey techniques.

Key words: damage estimation, prompt survey, SAR, Sediment Movement Magnitude, Sediment Disaster Scale

1. INTRODUCTION

Artificial satellite synthetic aperture radar (SAR) imagery (that can be obtained during bad weather and night conditions), has been used extensively for detecting large-scale landslides and landslide dams during several recent sediment disasters, including those caused by Typhoon Talas in the Kii Peninsula (in Japan, 2011) [*Hayashi et al.*, 2013a]; and Anbon Island (Indonesia, 2012) [*Mizuno et al.*, 2014]; as well as the Kumamoto earthquake (Japan, 2016) [*National Institute for Land and Infrastructure Management and Public Works Research Institute*, 2017].

Sediment disasters, including large-scale landslides and landslide dams, can cause large numbers of causalities and/or property damage (e.g. *Ishizuka et al.*, [2015]; *Tabata et al.*, [2002]). Estimating the maximum damage caused by a sediment disaster (hereafter called 'maximum damage') is an efficient means of assessing and managing risk. However, few previous studies have assessed methods for estimating the maximum damage. Using SAR imagery to estimate directly the maximum damage could help reduce the time required to determine essential resources for risk management and disaster mitigation.

Here we propose a method for estimating maximum damage using an index pertaining to sediment movement that is derived from SAR imagery. We evaluated the applicability of our method by comparing the estimated maximum damage with the actual damage, in addition to the time necessary for our method versus conventional disaster survey techniques.

2. METHOD USED TO ESTIMATE MAXIMUM DAMAGE

Our proposed method for estimating the maximum damage is shown in **Fig. 1**. Surveys utilizing SAR imagery were used to determine the area and location of landslides. We calculated the volume of sediment movement using the Guzzetti equation [*Guzzetti et al.*, 2009], based on the area of landslide:

$$V = 0.074A^{0.175} \quad (1)$$

where V is the volume of sediment movement (m^3), A is the area of landslide (m^2).

The relative height of sediment movement can be measured on a map using the location of landslide. The sediment movement magnitude (SMM) [*Uchida et al.*, 2005] can be calculated from volume and relative height, as follows:

$$SMM = log_{10} \sum_{i=1}^{n} (V_i H_i) \quad (2)$$

where V is the volume of sediment movement (m^3), and H is the relative height (m). The maximum damage is estimated using the Sediment Disaster Scale (SDS, **Fig. 2**) [*Hayashi et al.*, 2015]. SDS classifies sediment disasters into five categories using two indices - one that pertains to sediment movement (as SMM), and one that relates to the damage (as DL, [*Kojima et al.*, 2009]), which is based on the relationship between SMM and DL of past sediment disasters. DL is calculated using Eq. (3):

$$DL = 0.69\, log_{10}\, x_1 + 0.16\, log_{10} \left(x_2 + x_3 + \frac{x_4}{3}\right) + 1.07 \quad (3)$$

where x_1 is the number of persons killed or missing, x_2 is the number of persons injured, x_3 is the number of houses totally collapsed, and x_4 is the number of houses partially collapsed. SDS categories are defined as follows (excluding overlapping portions within the upper category):

Category I: SMM < 4.0 and DL < 1.0
Category II: 4.0 ≤ SMM < 6.0 or 1.0 ≤ DL < 1.5
Category III: 6.0 ≤ SMM < 8.0 or 1.5 ≤ DL < 2.0
Category IV: 8.0 ≤ SMM < 10.0 or 2.0 ≤ DL < 2.5
Category V: 10.0 ≤ SMM or 2.5 ≤ DL

According to *Hayashi* [2017], each SDS categories included typical sediment disasters as follows:

Category I: single slope failure
Category II: single slope failure or debris flow
Category III: multiple and/or simultaneous slope failure and/or debris flow
Category IV: single deep-rapid landslide and landslide dam
Category V: multiple and/or simultaneous deep-rapid landslides and landslide dams

3. SURVEY METHOD USING SAR IMAGERY

We included several examples of using SAR imagery surveys to detect large-scale landslides and landslide dams. **Fig. 3** shows the site locations and photos for each of the survey areas. We estimated the maximum damage by applying correlation coefficient difference analysis (CCDA, **Fig. 4**) [*Cao, et al.*, 2008] and normalized difference polarization index (NDPI) difference analysis (**Fig. 6**) [*Yamazaki et al.*, 2011] to areas affected by the 2008 Iwate-Miyagi inland earthquake (**Fig. 3a)**), the 2009 disaster in Hofu City caused by heavy rain (**Fig. 3b)**), [*Hayashi, et al.*, 2012] and by interpreting high-resolution SAR imagery to detect landslide dams in the Kii Peninsula that were affected by Typhoon Talas in 2011 (the Kii Peninsula Great Flood, **Fig. 3c)**) [*Hayashi et al.*, 2013b].

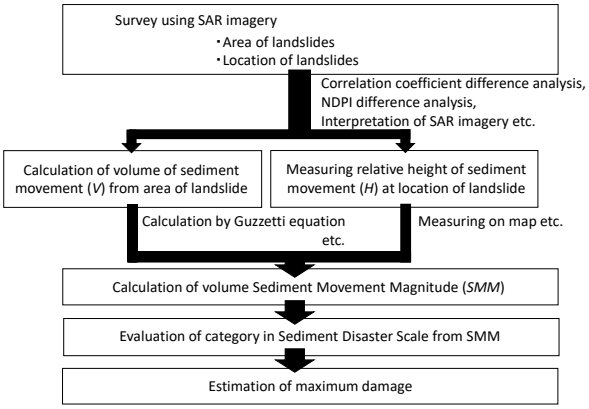

Fig. 1 Proposed method for estimating the maximum damage from synthetic aperture radar (SAR) imagery

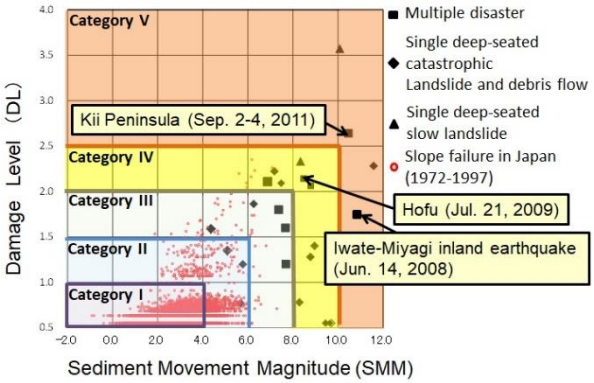

Fig. 2 Method of evaluating the Sediment Disaster Scale (SDS), based on *Hayashi et al.* [2015]

3.1 SAR imagery survey technique

Methods for detecting landslides that use SAR imagery taken before and after a disaster to calculate the difference and statistical value, or that are based on interpretation of SAR imagery, may reduce the time necessary for conducting these vital, time-sensitive surveys. Thus, we briefly review survey techniques that use SAR imagery to detect large-scale landslides and landslide dams.

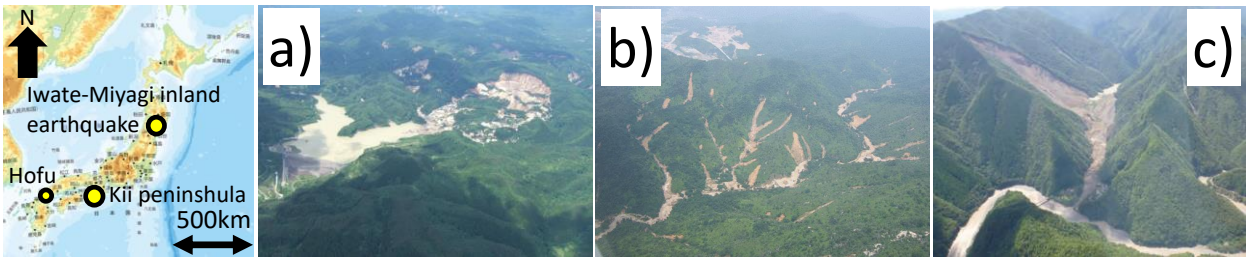

Fig. 3 Location map and photos of representative landslides within the survey areas: a) Iwate-Miyagi inland earthquake (Aratosawa landslide) [*Public Works Research Institute*, 2008], b) Hofu (Upper stream of Tsurugi River) and c) the Kii Peninsula Great Flood (Akadani landslide dam)

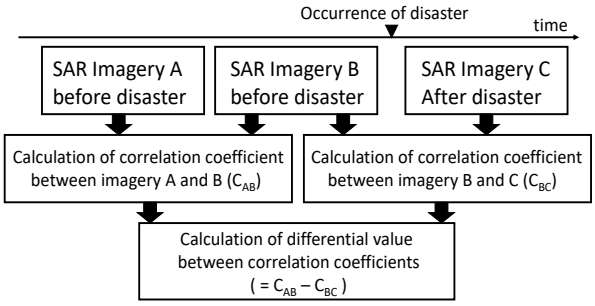

Fig. 4 Correlation coefficient difference analysis procedure

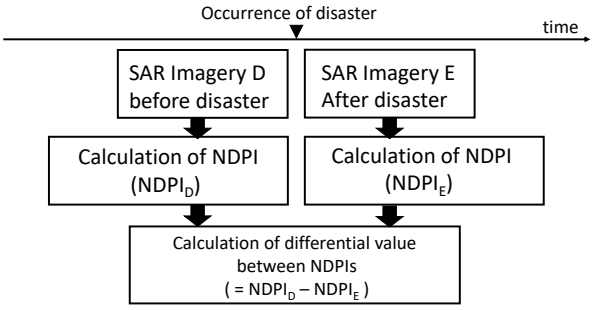

Fig. 6 NDPI defference analysis procedure

Table 1 List of SAR images for CCDA in *Hayashi et al.* [2012]

Name of disaster (Date of disaster occurrence)	Artificial satellite, Band, Polarization mode	Date of acquisition
Iwate-Miyagi inland earthquake (2008/6/14)	ALOS, L band, HH	2007/8/29 2008/5/31 2008/7/16
Hofu (2009/7/21)		2007/10/9 2009/7/14 2009/8/12

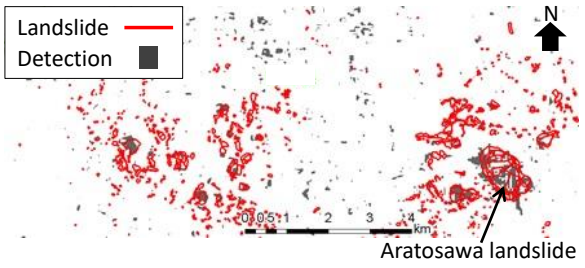

Fig. 5 The example of the result of CCDA against Iwate-Miyagi inland earthquake after *Hayashi et al.* [2012] (Red line indicates landslide interpreted by aerial photograph, Gray dot indicates detection result of CCDA)

Table 2 List of SAR images for NDPI difference analysis in *Hayashi et al.* [2012]

Name of disaster (Date of disaster occurrence)	Artificial satellite, Band, Polarization mode	Date of acquisition
Iwate-Miyagi inland earthquake (2008/6/14)	ALOS, L band, HH+HV	2007/6/21 2008/9/23
Hofu (2009/7/21)		2009/7/14 2009/8/12

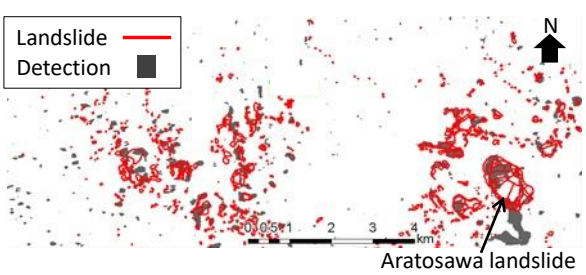

Fig. 7 The example of the result of NDPI difference analysis against Iwate-Miyagi inland earthquake after *Hayashi et al.* [2012] (Red line indicates landslide interpreted by aerial photograph, Gray dot indicates detection result of NDPI difference analysis)

3.2 CCDA

CCDA [*Cao, et al.*, 2008] is used to detect landslides using single-polarization SAR imagery (as shown in **Fig. 4**). CCDA uses three SAR images: two that are taken prior to the disaster (SAR images A and B) and one taken after the disaster (SAR image C). Correlation coefficients are calculated between SAR images A and B (C_{AB}), and SAR images B and C (C_{BC}). The difference value between C_{AB} and C_{BC} indicates potential landslide areas; the larger the value the more likely a landslide is to occur. According to *Hayashi et al.* [2012], the landslide area must be larger than 40,000 m^2 to be able to detect a landslide with 100% accuracy using CCDA. **Table 1** shows list of SAR images for

CCDA and **Fig. 5** shows the example of the result of CCDA in *Hayashi et al.* [2012].

3.3 NDPI difference analysis

NDPI difference analysis [*Yamazaki et al.*, 2011] is one of the methods used for detecting landslides using dual-polarization SAR imagery. NDPI difference analysis procedure is shown in **Fig. 6**. NDPI difference analysis uses two SAR images, one before and one after a disaster (SAR images D and E, respectively). For each SAR image, the NDPI is calculated as $NDPI_D$ and $NDPI_E$. The NDPI is defined as

$$NDPI = \frac{(HH-HV)}{(HH+HV)} \quad (4)$$

where *HH* is the horizontal transmit and the horizontal receive, *HV* is the horizontal transmit and the vertical receive. $NDPI_D$ and $NDPI_E$ values are then used to calculate the difference value; a large difference value indicates likely landslide candidates. According to *Hayashi et al.* [2012], the area of the landslide resulting from the Iwate-Miyagi inland earthquake was larger than 62,500 m^2, and 40,000 m^2 in Hofu, which is sufficiently large for NDPI difference analysis with 100% accuracy. **Table 2** shows list of SAR images for NDPI difference analysis and **Fig. 7** shows the example of the result of NDPI difference analysis in *Hayashi et al.* [2012].

3.4 Interpretation of high-resolution SAR imagery

To detect landslide dams, authors examined a high-resolution SAR imagery obtained using TerraSAR-X (X band, 2011/9/5), mainly from the southern part of the Nara Prefecture, for sediment disasters associated with the Kii Peninsula Great Flood (Date of disaster occurrence: 2011/8/31 to 9/4) [*Hayashi et al.*, 2013b]. Typical landslide dam shapes within a SAR images were identified, including lakes formed by landslide dams, landslide scarps and stream blockages. **Fig. 8** shows the example of interpretation of high-resolution SAR imagery in *Hayashi et al.* [2013b].

4. RESULTS AND DISCUSSION

We compared the maximum damage estimated by our method with the actual evaluated damages based on disaster records (**Fig. 2**). We also compared the time necessary using our proposed method with the time needed for conventional disaster survey techniques for sediment disasters caused by the Great East Japan Earthquake and the Great Flood in the Kii Peninsula [*Hayashi, et al.*, 2017].

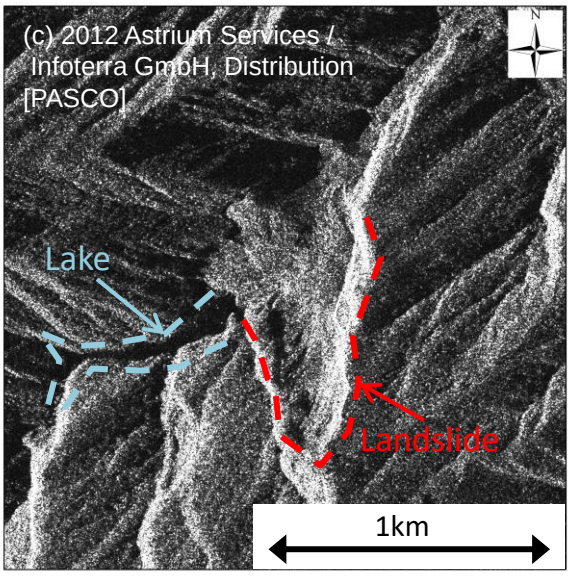

Fig. 8 The example of interpretation of high-resolution SAR imagery against the Kii Peninsula Great Flood after *Hayashi et al.* [2013b] (Akadani landslide dam)

4.1 Calculation of SMM and DL and SDS evaluation against actual damage

SMM and DL values from the actual damage were calculated for the Iwate-Miyagi inland earthquake based on disaster records [*Miyagi Prefecture*, 2008; *The Japanese Geotechnical Society*, 2010]. Values of SMM and DL were calculated both for Hofu, *Hayashi et al.* [2010], and the Great Flood in the Kii Peninsula, *Hayashi et al.* [2015]. The Iwate-Miyagi inland earthquake and the Kii Peninsula Great Flood were evaluated as category V, and Hofu evaluated as category IV (according to SDS category), as shown in **Fig. 2**.

4.2 Calculation of SMM and DL from SAR imagery

SMM can be calculated by our proposed method from SAR imagery. **Table 3** shows SMM values calculated by CCDA and NDPI difference analysis results from the Iwate-Miyagi inland earthquake and the Hofu disaster. Here, the area and number of landslides accurately detected by CCDA and NDPI difference analysis were identified; the relative height was 100 m with reference to the height difference between the altitude of the surrounding mountains and the riverbed. **Table 4** shows SMM values calculated by interpretation of SAR imagery from the Kii Peninsula Great Flood. *Hayashi et al.* [2013b] presented the location and area of large-scale landslides that caused landslide dams, where the relative heights were measured by *GSI Maps* [2017].

Table 3 SMM calculated by CCDA and NDPI (SMM: sediment movement magnitude; CCDA: correlation coefficient difference analysis; NDPI: NDPI difference analysis)

Name of disasters	Analysys method	Area of landslide per one landslide (m^2)	Volume of landslide per one landslide (m^3)	Provisional relative height (m)	Number of detedted landslide	SMM
Iwate-miyagi inland earthquale	CCDA	40,000	348,513	100	13	8.66
	NDPI	62,500	665,668	100	9	8.78
Hofu	CCDA	40,000	348,513	100	26	8.96
	NDPI	40,000	348,513	100	24	8.92

Table 4 SMM calculated by interpretation of SAR imagery

Name of landslide	Area (ha)	Volume of sediment movement (m^3)	Relative height (m)	SMM
Tsubonouchi-1	2.0	127,563	180	7.36
Tsubonouchi-2	11.8	1,672,864	180	8.48
Tsubonouchi-3	5.2	509,843	200	8.01
Ui	8.7	1,075,312	230	8.39
Nagatono	19.5	3,465,628	440	9.18
Akadani	28.2	5,916,882	570	9.53
Kuridaira	33.7	7,661,170	330	9.40
Mikoshi	6.3	673,404	180	8.08
All				9.91

Table 5 Comparison between SMM and SDS derived from actual damage and results of our estimation

Name of disaster	Analysys method	Result of estimation		Actual damage	
		SMM	Category	SMM	Category
Iwate-miyagi inland earthquale	CCDA	8.66	Ⅳ	10.37	Ⅴ
	NDPI	8.78	Ⅳ		
Hofu	CCDA	8.96	Ⅳ	8.48	Ⅳ
	NDPI	8.92	Ⅳ		
The Great Flood in the Kii Peninsula	Interpretation	9.91	Ⅳ	10.46	Ⅴ

4.3 Comparing actual damage to estimated maximum damage based on SDS

Table 5 shows results from comparing the maximum damage estimated by our proposed method (**4.2**) to the actual damage (**4.1**). Our method underestimated values for the Iwate-Miyagi inland earthquake compared with values of the actual damage. This was because the Aratosawa landslide (which was approximately 70 million m^3) increased the actual damage; this landslide was undetected by CCDA and NDPI difference analysis, as the precise landslide area could not be estimated. In Hofu, the estimated and actual damage were very close for SMM values, with the same SDS categories. For the Great Flood in the Kii Peninsula, values of SMM were close, despite the presence of the Iya deep-rapid landslide (which was approximately 4.1 million m^3) and the town of Nachi-katsuura (where simultaneous debris flows occurred) were outside of the SAR imagery interpretation area [*Hayashi et al.*, 2013b]. Because values of SMM straddle SDS category delineations, the SDS category that results from our estimation is one category lower than that derived from the actual damage. Thus, we confirmed the applicability of our proposed method as the maximum estimated damage is nearly the same as the actual damage. However, our proposed method may underestimate the maximum damage if a huge landslide (such as the Aratosawa landslide during the Iwate-Miyagi

earthquake) occurs within the SAR imagery area, due to the accuracy of the analysis method necessary to detect such landslides.

4.4 Comparing the survey time

Surveys for CCDA and NDPI difference analysis required 11.5 hours per ~300 km^2 [*Hayashi, et al.*, 2012], which equates to approximately 630 km^2/day. Interpretation of SAR imagery can survey 1,200 km^2/day [*Hayashi, et al.*, 2017]. If the location and area of landslides are determined by surveys using SAR imagery, SMM and SDS can be calculated promptly. Emergency inspections (EI) for high-risk areas to prevent secondary damage are conducted in Japan by special teams from the Ministry of Land, Infrastructure, Transport and Tourism (MLIT) and prefectural governments (PG) (i.e. *Minami and Osanai, et al.*, [2014]). EI can survey ~630 km^2/day [*Hayashi, et al.*, 2017], and offers the most immediate method of surveying large-scale sediment disasters. While our proposed method could be conducted even during bad weather and at night, EI is typically not conducted during such conditions. As a result, the proposed method can be conducted over a wider range of conditions, creating more opportunities to conduct surveys than EI.

5. CONCLUSIONS

In this study, we proposed a method to estimate maximum damage based on SDS using SAR imagery. This study evaluated and confirmed the applicability of this method, demonstrating that it could reduce the time necessary for surveying after a disaster. Our proposed method was validated using SMM values, in which the SDS category estimated by our proposed method was nearly that of actual damage from several past disasters. However, our method underestimated the maximum damage when a huge landslide (such as the Aratosawa landslide from the Iwate-Miyagi inland earthquake) was located in the SAR imagery. Significantly, our method can reduce the time necessary for surveying compared with conventional disaster survey techniques.

We did not compare our method to other analysis methods that use SAR imagery to detect landslides, and consider the time affected by cycle, return time, and satellite location to obtain SAR imagery. Therefore, further examination is necessary to improve our proposed method, specifically towards refining imagery detection accuracy (for determining the size and location of landslides), and improving the time necessary to obtain SAR imagery critical for estimating the maximum damage.

REFERENCES

Cao, Y., Yan, L., and Zheng, Z. (2008): Extraction of information on geology hazard from multi-polarization SAR images, XXIst International Society for Photogrammetry and Remote Sensing Congress, XXXVII-B4, pp. 1529-1532.

GSI Maps (2017): https://maps.gsi.go.jp/

Guzzetti, F., Ardizzone, F., Cardinali, M., Rossi M. and Valigi, D. (2009): Landslide volumes and landslide mobilization rates in Umbria, central Italy, Earth and Planetary Science Letters, Vol. 279, pp. 222-229.

Hayashi, S. (2017): A study for prompt survey techniques against large-scale sediment disaster, doctoral thesis, Hokkaido Univ., 135pp. (in Japanese).

Hayashi, S., Mizuno, M., Osanai, N., Nishi, M., Shimizu, Y. Nakagawa, K. and Matsumoto, S. (2012): Applicability of methods for detecting landslides by using synthetic aperture radar of ALOS (Daichi), Journal of the Japan Society of Erosion Control Engineering, Vol.65, No.4, pp.3-14 (in Japanese with English abstract).

Hayashi, S., Mizuno, M. Sato, T., Kamiyama, J., Okamoto, A., Yoshikawa, T., Udono, T., Yokota, H., Noda, A. and Yoshikawa, K. (2013b): Establishing a landslide dam detection methodology by interpreting artificial satellite high‐resolution SAR（synthetic aperture radar）images based on a case study of sediment-related disasters caused by Typhoon Talas in the Kii Peninsula, Journal of the Japan Society of Erosion Control Engineering, Vol.66, No.3, pp.32-39 (in Japanese with English abstract).

Hayashi, S., Osanai, N., Shimizu, Y., Nakata, M. Matsuda, M. and Ogawa, K. (2010): Study on the scale of sediment disasters caused in Hofu, Yamaguchi, Proceedings of the 59th Research Meeting of the Japan Society of Erosion Control Engineering, pp. 266-267 (in Japanese).

Hayashi, S., Uchida, T., Katsura, S., Kasai, M., Osanai, N. and Marutani, T. (2017): A quantitative analysis of emergency survey techniques for large-scale sediment disasters, Journal of the Japan Landslide Society, Vol.54, No.2, pp.18-25 (in Japanese).

Hayashi, S., Uchida, T., Okamoto, A., Ishizuka, T., Yamakoshi, T. and Morita, K. (2013a): Countermeasures against landslide dams caused by typhoon Talas 2011, Asia-Pacific Tech Monitor, Vol. 30, No. 1, pp. 20-26.

Hayashi, S., Uchida, T., Okamoto, A., Osanai N., Lee, C. and Woo, C. (2015)：Estimation of the socio-Economic impacts of sediment disasters by using evaluation indexes of the magnitude of sediment movement and level of damage to society, International Journal of Erosion Control Engineering Vol. 8, No. 1, pp. 1-10.

Ishizuka, T., Tokunaga, Y. and Sawano, H. (2015): Activities toward a landslide dam outburst flood in Ambon Island, Indonesia, Journal of Japan Society of Civil Engineers, Division F, Vol. 71, No. 2, pp. 24-32 (in Japanese with English abstract).

Kojima, S., Osanai, N., Nishimoto, H., Ogawa, K. and Matsuda, M. (2009): Study of damage indices based on questionnaire surveys of the damage image of sediment disasters, Journal of the Japan Society of Erosion Control Engineering, Vol. 62, No. 3, pp. 47-54 (in Japanese with English abstract).

Minami, N. and Osanai, N. (2014): Introduction to modern SABO studies, Kokon Shoin, 184pp. (in Japanese).

Miyagi Prefecture (2008): The final report of the technical committee for sediment-related disasters caused by the Iwate-Miyagi inland earthquake, 101pp. (in Japanese).

Mizuno, M., Kamiyama, J., Ekawa, M., Kanbara, J., Hayashi, S., Morita, K., Horiuchi, S., Udono, T. and Yoshikawa, K. (2014): Application of high-Resolution SAR satellite images to landslide disasters -Report on landslide-dam formation and collapse events in the Kii Peninsula, Japan and Ambon, Indonesia- , Proceedings of the INTERPAEVENT 2014 in the Pacific Rim, pp. 362-371.

National Institute for Land and Infrastructure Management and Public Works Research Institute (2017): Report on damage to infrastructures by the 2016 Kumamoto earthquake, Technical note of National Institute for Land and Infrastructure Management No. 967, Technical note of Public Works Research Institute No. 4359, 356pp. (in Japanese).

Public Works Research Institute (2008): Landslides and slope collapses triggered by Iwate-Miyagi Nairiku earthquake, https://www.pwri.go.jp/team/landslide/english%20pages/topics/topics_iwatemiyagi_e.htm

The Japanese Geotechnical Society (2010): The disaster report of the Iwate-Miyagi inland earthquake, 2008, 159pp. (in Japanese).

Tabata, S., Mizuyama, T. and Inoue, K. (2002): Landslide Dams and Disasters, Kokon Shoin, 205pp. (in Japanese).

Uchida, T., Kunitomo, M., Terada, H., Ogawa, K. and Matsuda, M. (2005): Study of methods of representing the scale of sediment disasters, Journal of the Japan Society of Erosion Control Engineering, Vol. 57, No. 6, pp. 51-55 (in Japanese with English abstract).

Yamazaki, F., Liu, W. and Inoue, H. (2011): Characteristics of SAR backscattered intensity and its application to earthquake damage detection, Computational Stochastic Mechanics, pp. 602-606.